Thin-film ferroelectric microwave devices

Supercond. Sci. Technol. **11** (1998) 1323–1334. Printed in the UK PII: S0953-2048(98)96246-7

Thin-film ferroelectric microwave devices

M J Lancaster, J Powell and A Porch

The University of Birmingham, School of Electronic and Electrical Engineering, Edgbaston, Birmingham B15 2TT, UK

Received 27 July 1998

Abstract. When an electric field is applied to a ferroelectric material, the microwave permittivity undergoes a substantial change. This change in permittivity can be utilized in microwave devices to produce frequency-agile functions. This paper is a comprehensive review of the work on ferroelectric materials; this includes models of the ferroelectric permittivity and loss tangent, as well as methods of measurement of these properties. New measurements are presented on thin-film strontium titanate and single-crystal strontium barium titanate substrates. These results are compared with the model. A brief discussion is given of the applications of ferroelectric material in microwave devices.

1. Introduction

Ferroelectrics have been studied for many years and have been found to be particularly important materials for application in piezoelectric, pyroelectric, electrostrictive and linear and nonlinear optical devices. This paper is about the more recent studies on the use of ferroelectrics in the microwave region of the electromagnetic spectrum. The main interest here is that the dielectric constant of some ferroelectric materials can change substantially with the application of an electric field. This paper gives an overview of the development of ferroelectric materials for microwave applications, a review of the current state of the art in both materials and devices, and some new measurements on the properties of thin-film strontium titanate (STO) and single-crystal strontium barium titanate (SBT).

A ferroelectric material exhibits spontaneous polarization. A crystal of such a material consists of positive and negative ions, and in a certain temperature range the positive and negative ions become displaced. The displacement results in a net dipole moment. The orientation of the dipole moment in a ferroelectric can be shifted from one orientation to another by the application of an electric field. The appearance of the spontaneous polarization is highly temperature dependent and, in general, ferroelectric crystals undergo phase transitions which involve structural changes. As the temperature decreases from above the Curie temperature, a structural phase change takes place and the crystal changes from paraelectric to ferroelectric [1]. An example of such a material is $BaTiO_3$, which has a Curie temperature of 120 °C. Because of the nature of the crystal structure close to the Curie temperature, the thermodynamic properties show large anomalies. This is usually the case with the dielectric constant, which increases to a large value close to the Curie temperature. For temperatures above the Curie temperature, the Curie–Weiss law describes the temperature dependence of the dielectric constant for many ferroelectrics. The dielectric constant is given by $\varepsilon = \varepsilon_{CW} + C_{CW}/(T - T_{CW})$. Here ε_{CW}, C_{CW} and T_{cw} are constants. In this region the dielectric constant is most sensitive to the magnitude of the applied electric field.

Ferroelectrics have been studied since the early 1960s for application in microwave devices [2, 3], and their properties have since been studied extensively. However, it is only relatively recently that applications are beginning to emerge. This recent renewed interest is due to a number of factors, one being their compatibility with high-temperature superconductors in terms of their final application and similar methods of production. The change in dielectric constant as a function of electric field is the key to a wide range of applications.

Examples of applications in the field of microwave engineering include field-dependent capacitors, tunable resonators, phase shifters, frequency-agile filters, variable-power dividers and variable-frequency oscillators. Nonlinear applications such as harmonic generation, pulse shaping, mixing and parametric amplification are also a possibility. Such components have a wide range of applications in many communication and radar systems. For example, variable-phase shifters, one of the first and simplest components to be made with ferroelectrics, are used in antenna arrays in order to produce a beam scanning function. It is possible to integrate ferroelectric materials to produce complex electronically steerable antenna arrays with applications in both military and commercial radar and communication systems. Electronically controlled filters can be produced with applications of interference suppression, secure communications, dynamic channel allocation, signal jamming and satellite and ground-based communications switching. Many new systems concepts will appear as high-performance materials emerge, and

0953-2048/98/111323+12$19.50

these systems will have considerably improved performance over conventional systems. A non-microwave application that has received a great deal of interest recently is computer memory devices.

There are other methods of producing the tunable components described above. For example, devices fabricated using ferrite materials have been used for many years and continue to be investigated; in addition PIN diodes also produce similar functions. In comparison with the ferroelectric devices, ferrite devices are generally large, heavy and slow and have a large power consumption, although recent interest in using superconductors [4] in combination with these devices improves on some of these disadvantages. PIN diode devices are inexpensive but have a high insertion loss and are slower. It is possible to produce a phase shifter using superconductors alone since the kinetic inductance of the electron pairs increases on the application of a dc magnetic field, dc bias current, increased temperature or optical irradiation. A change in kinetic inductance produces a change in velocity on a transmission line, giving a phase shift. However the effect is usually small and also results in an increase in the loss of the transmission line [5]. Phase shifters based on arrays of junctions in the form of SQUIDs have been produced, but the power handling of these devices is very limited [6]. More recently, interest has emerged in micro electromechanical systems (MEMS), where tunability is obtained by the physical movement of a component, for example to change the capacitance of the device. Such systems can be very small and use electrostatic, electrostrictive, piezoelectric or thermal effects to produce the movement [7].

Ferroelectric devices are fast, small and lightweight and, because they work using an electric field, have low power consumption. The range of tuning is quite large and devices are relatively simple in nature. The small size of the ferroelectric components, mainly as a result of the high dielectric constants involved, can produce a high conductor loss in circuits, but if superconductors are the conductor loss is essentially eliminated in such small devices [5]. The main problems currently being addressed are the relatively high loss tangents of the practical ferroelectric materials and the large bias voltages required. The latter can be tackled by novel device structures, provided that the breakdown strength of the materials is sufficiently high.

2. Materials

Some materials which have shown a variable permittivity with electric field are $SrTiO_3$, $(Ba, Sr)TiO_3$, $(Pb, Sr)TiO_3$, $(Pb, Ca)TiO_3$, Ba $(Ti, Sn)O_3$, Ba $(Ti, Zr)O_3$ and $KTaO_3$. Dopants are introduced into pure STO to attempt to improve the microwave properties, and there has been some success at reducing the loss tangent [8–10].

By far the most studied material for microwave applications is $Sr_{1-x}Ba_xTiO_3$ (SBT), where x can vary from 0 to 1. $SrTiO_3$ (STO) is of particular interest because of its crystalline compatibility with high-temperature superconductors (HTSs) and its properties at low temperature. Pure STO is paraelectric for all

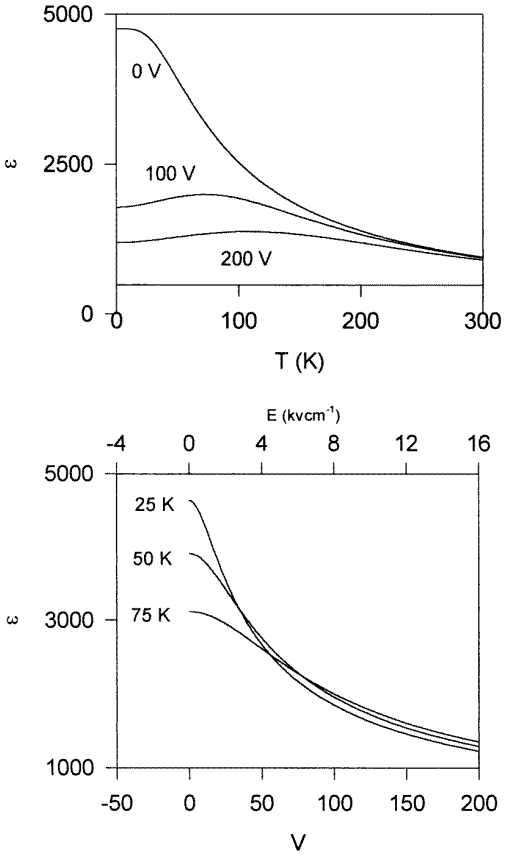

Figure 1. Variation of the dielectric constant of STO as a function of electric field and temperature. (The parameters used to fit these data are as follows: Curie temperature, T_C = 25 K; sublattice 'Debye' temperature, Θ = 152 K, zero-temperature permittivity, ε_{00} = 12 000; normalizing electric field, E_N = 1 kV cm^{-1}; dispersion parameter, characterizing sample inhomogeneity, ξ_{st} = 0.8.)

temperatures; there is no Curie temperature above 0 K. Some thin films and amorphous ceramic forms show a low-temperature peak in the dielectric constant, implying that the Curie temperature is above 0 K, probably because of stresses or impurities in the films. For SBT, as the value of x varies from 0 to 1, the Curie temperature varies from the value of pure STO to about 400 K, the Curie temperature of $BaTiO_3$ (BTO). This allows tailoring of the Curie temperature; generally a value of $x = 0.5$ is used to optimize its properties for room temperature, and a value of around 0.1 used when the material is to be used in conjunction with HTS films.

The electric field and temperature dependences of the dielectric constant of an $Sr_{0.97}Ba_{0.03}TiO$ single-crystal substrate are plotted in figure 1. These data were generated using the phenomenological model developed by Vendik [11], described later in this paper, with material parameters chosen to reflect the dielectric constant extracted from coplanar resonator measurements presented later and shown in figure 9. The very large values of the permittivity should be noted.

There are a number of different forms of ferroelectric materials that are of interest for applications. Single

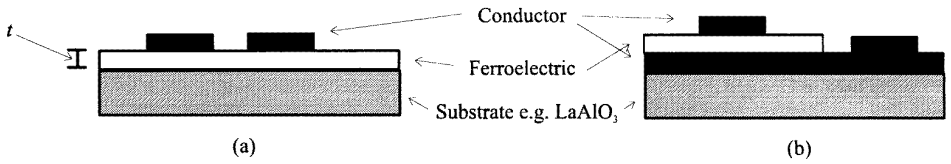

Figure 2. Measurement of low-frequency properties of films by (*a*) coplanar capacitor and (*b*) parallel-plate capacitor.

crystals have been studied for many years [12], and more recently thin films of the materials have been studied; these films are almost exclusively made by laser ablation and are usually less than 1 μm thick. The films are also predominantly deposited on $LaAlO_3$ substrates and are usually single layers, with an HTS or a normal conductor placed on the top surface. However, trilayer films have also been produced, forming an HTS/ferroelectric/HTS structure. Films on sapphire have also been produced with a CeO_2 buffer layer to compensate for the lattice and thermal expansion mismatch [13]. In addition, non-crystalline bulk ceramic forms have been produced; for example, the microwave losses and dispersion of the dielectric constant of polycrystalline BTO were studied extensively in the 1960s [14]. However, the Curie temperature of BTO is rather large for practical applications. The sol–gel technique [15] for producing BST has been developed more recently. This technique is able to produce material that is of the order of 0.1 mm thick. A promising material has also been developed which is a combination of SBT and MgO in a ceramic form [16].

3. Low-frequency properties

There are essentially two structures for measuring the dc or low-frequency properties of films; the coplanar capacitor or the parallel plate capacitor. Figure 2 shows these two geometries, although in the literature there are some variations in the exact configurations. Single-crystal and ceramic plate measurements adopt similar geometries, with larger thickness t and of course no substrate.

The shape of the surface electrode is important for determining the capacitance of the structure, and for the parallel-plate configuration it is generally square or rectangular. The capacitance is usually fairly large owing to the thickness of the ferroelectric film being small. For the coplanar structure [17–20] the electrodes need to be close together to maximize the field within the ferroelectric. An interdigital finger structure can be used to increase the capacitance [21, 22]. The properties of the ferroelectric materials can be extracted from the measured capacitance and dielectric losses using a conformal mapping technique, such as that described below [23].

There have been quite a large number of capacitive measurements of the dielectric properties of SBT and STO from a range of groups worldwide. Measurements of the dielectric constant and loss tangent of STO and SBT thin films and single crystals are not necessarily very consistent between manufacturers, owing to the differing quality of the materials. Measurements are typically performed at frequencies between 100 kHz and 1 MHz. The loss tangent of STO single crystals is of the order 2×10^{-4} at 77 K [24], but in the thin-film forms this is much bigger and almost all manufacturers quote loss tangents in the range 0.01–0.1 [17, 19]. This high loss tangent also applies to SBT thin films, irrespective of their composition [15, 18, 19, 23, 25]. This is probably the main area of concern in the development of ferroelectric films for microwave applications, where the losses need to be reduced further if such films are to be used in the widespread applications mentioned previously. The tunability at low frequencies also varies between different film manufacturers, but can be 50% and above. This occurs with low voltages with the trilayer structure, but larger voltages are required in structures where the applied voltage is across a larger distance. A similar tuning range has also been observed in SBT thin films [18] and sol–gel produced [15] material at room temperature; here the materials have approximately equal amounts of strontium to barium in order to increase the Curie temperature. Problems with the quality of the thin films have been put down to compositional inhomogeneities and interface effects, including stresses and internal fields in the materials, producing an asymmetry in the positive and negative bias response.

Modelling the microwave dielectric properties of ferroelectric materials, and in particular the physical mechanisms underlying the temperature, electric field and frequency dependences of ε and $\tan\delta$ has been discussed extensively since the late 1950s [26, 27]. It is not our intention to discuss these models here. A phenomenological model of the permittivity and losses of ferroelectrics has been developed by Vendik [11] and subsequently discussed by Gevorgian *et al* [28]. The model produces the following expression for the relative dielectric constant ε as a function of temperature T and small electric field E:

$$\varepsilon(E,T) = \frac{\varepsilon_{00}}{\Phi(E,T)} \tag{1}$$

where

$$\Phi(E,T) = [(\xi^2+\eta^3)^{1/2}+\xi]^{2/3} + [(\xi^2+\eta^3)^{1/2}-\xi]^{2/3} - \eta$$

$$\xi(E) = \left[\left(\frac{E}{E_N}\right)^2 + \xi_{st}^2\right]^{1/2}$$

$$\eta(T) = \frac{\Theta}{T_0}\left[\frac{1}{16} + \left(\frac{T}{\Theta}\right)^2\right]^{1/2} - 1.$$

Here, E_N is the normalizing bias field, ξ_{st} the rate of crystal strain, a measure of the density of defects, T_0 the Curie temperature, ε_{00} is a constant analogous to the Curie constant and Θ the Debye temperature. It is possible to use these parameters to fit experimental measurements

to the model. The change of ε with frequency is small in the microwave frequency range. The losses in a ferroelectric crystal are more difficult to analyse since they originate from three predominant sources [11, 29], namely (1) a fundamental loss associated with multiphonon scattering, (2) a loss associated with the conversion of the microwave field into acoustic oscillations by regions with residual ferroelectric polarization and (3) a loss due to charged defects converting the microwave field into acoustic oscillations. The loss tangent is given by the sum of these different loss mechanisms [29], i.e.

$$\tan\delta = \tan\delta_1 + \tan\delta_2 + \tan\delta_3. \qquad (2)$$

The individual loss tangents with respect to the above list of loss mechanisms are

$$\tan\delta_1 = A_1\left(\frac{T}{T_0}\right)^2 \frac{1}{\Phi(E,T)^{3/2}}$$

$$\text{where } A_1 = \frac{\pi}{8}\frac{\omega_{00}}{\omega_M}\frac{\omega}{\omega_{00}}$$

$$\tan\delta_2 = A_2 Y(E,T)^2 \frac{1}{\Phi(E,T)}$$

$$\tan\delta_3 = A_3 n_d \frac{1}{\Phi(E,T)}$$

where

$$Y(E,T) = [(\xi^2+\eta^3)^{1/2}+\xi]^{1/3} + [(\xi^2+\eta^3)^{1/2}-\xi]^{1/3}.$$

Here A_1, A_2, A_3 are material parameters, Y is a normalized parameter of the ferroelectric polarization and n_d is the density of charged defects. For high-quality crystals, $\tan\delta_3$ is small and the other two loss mechanisms dominate; however, for thin films the defect density may be significant and this term becomes more important.

In figure 3 the loss tangent is plotted, calculated using equation (1) and equation (2). Figures 3(a) and 3(b) show the temperature and electric field dependences of the loss tangent, where the model parameters are chosen to reflect the coplanar resonator measurements of an $Sr_{0.97}Ba_{0.03}TiO$ single-crystal substrate (see figure 9). In this case, contributions to the loss tangent due to fundamental losses (multiphonon scattering) and acoustic oscillations due to residual polarization are plotted, together with the total loss tangent. The material fitting parameters used were $A_1 = 10^{-4}$ and $A_2 = 4\times10^{-4}$. In figure 3 (c) the electric field dependence of the loss tangent is plotted, where the material parameters are chosen to represent the coplanar resonator measurements of thin-film bilayers (see figure 9). Here we have included the effects due to charged defects. The material fitting parameters used were $A_1 = 0.6$, $A_2 = 1$ and $A_3 = 2$, yielding a total loss tangent over three orders of magnitude larger than that found for the single-crystal substrate plotted in figure 3(b). We also note that the bilayer and single-crystal data display an opposite dependence on the electric field, arising from the interplay of the competing loss mechanisms. In each case, other material parameters have been set at those used to simulate the dielectric constant data shown in figure 1.

For the permittivity, this model predicts the same form for the bias field and temperature dependence of the permittivity as that reported for the SBT single-crystal measurements, shown in figure 1. However, thin-film

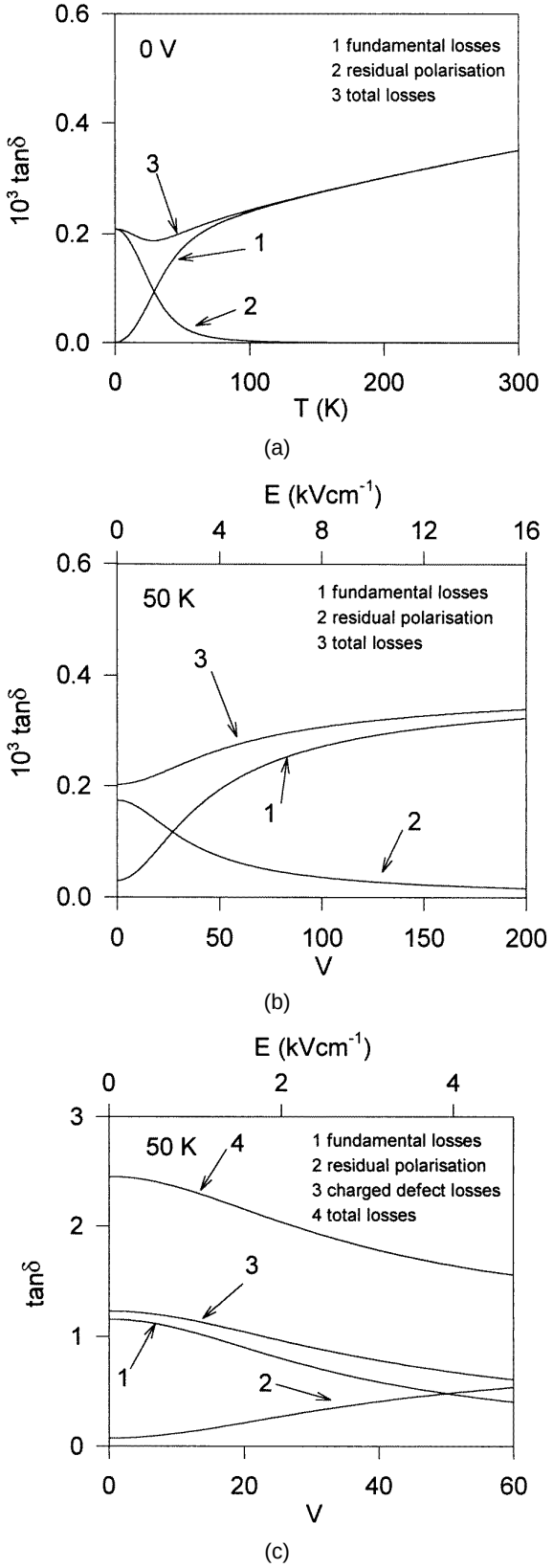

Figure 3. Modelled loss tangent for an SBT single crystal.

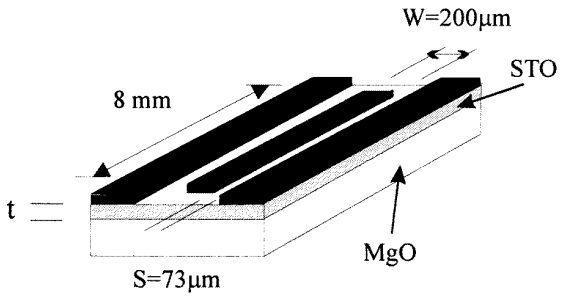

Figure 4. Coplanar resonator on the surface of an STO thin film.

measurements yield absolute values for ε around a factor of 5 lower than those for the single-crystal measurements. Such differences undoubtedly arise from crystalline defects, which are usually much more prevalent in the thin-film samples. Wide variations in absolute values of ε, which we have determined experimentally for thin-film and single-crystal samples, will be discussed in the following section.

4. Measurement of microwave properties

Measurements of the dielectric properties of ferroelectrics at microwave frequencies are performed by the use of either resonators or transmission lines. When using a resonator, observing the centre frequency and quality factor provides information about the dielectric constant and loss tangent. When using a transmission line, observing the delay and line attenuation provides similar information. The key to these measurements is the deconvolution of the resonator geometry from the measurement, removing the effects of other dielectrics in the resonator, as well as other loss mechanisms. A number of different types of resonator have been used based on the coplanar or microstrip structures with cross-sections similar to those in figure 2, and these are discussed briefly below.

4.1. Coplanar geometry

The coplanar geometry is probably the most widely used characterization tool for ferroelectric films and substrates [30–33]. This is because it requires only one layer of metallization. A simple coplanar resonator [34] is shown in figure 4, which consists of a length of coplanar transmission line open circuit at both ends. There is a ground plane at each side of the central conductor. This metal or HTS structure is deposited on the surface of the thin film of ferroelectric, which in turn has been deposited on the surface of the substrate. In order to apply a dc bias, the ground planes can be electrically separated and a voltage applied between them; alternatively an external bias T can be used.

The key to the determination of the dielectric properties of the ferroelectric thin film depicted in figure 4 is the calculation of the effective dielectric constant, which is a combination of the dielectric constant of the air above the resonator, the ferroelectric film and the substrate material. This effective dielectric constant ε_{eff} determines the velocity c of the wave on the coplanar transmission line since $c = 1/(\varepsilon_{eff}\varepsilon_0\mu)^{1/2}$ which in turn is related to the resonant frequency of the resonator $f = c/2l$ or the delay along a coplanar transmission line l/c of length l. In general, the effective length of the transmission line is longer than its physical length owing to fringing field effects which result from the extension of the electromagnetic field past the end of the resonator. Uncertainties in parameters extracted from such measurements can be eliminated by performing multiple measurements using several device geometries. Conformal mapping techniques have been used to analyse coplanar waveguides on the surface of a semi-infinite dielectric sheet and have proved successful in developing expressions for the effective dielectric constant and impedance of a coplanar transmission line [35–39]. More recently, these techniques have been developed for the determination of the properties of the coplanar line shown in figure 4 [40–43].

An expression for the effective dielectric constant for the structure with dimensions defined in figure 4 is given by [41]

$$\varepsilon_{eff} = 1 + q_1(\varepsilon_1 - \varepsilon_2) + q_2(\varepsilon_2 - 1)/2. \qquad (3)$$

The dielectric filling factors for the ferroelectric film ($i = 1$) and the substrate ($i = 2$) are given by

$$q_i = \frac{K(k_i)}{K(k_i')}\frac{K(k_0')}{K(k_0)}$$

where K is the complete elliptic integral of the first kind with

$$k_0 = \frac{W}{W + S/2} \qquad k_i = \frac{\sinh(\pi W/2h_i)}{\sinh[\pi(W/2 + g)/2h_i]}$$

and

$$k_i' = (1 - k_i^2)^{1/2}.$$

Some computational difficulties may be encountered when attempting to evaluate dielectric filling factors for the ferroelectric layers, where the ratio of the line dimensions to the layer thickness becomes extremely large. In this case the limiting form

$$q_i = \frac{\pi}{\ln(16) + \pi g/h_i}\frac{K(k_0')}{K(k_0)}$$

can be employed, which is accurate to better than 1% for $W/h_i > 1$.

The losses in the ferroelectric film can also be deduced, assuming that the losses in the HTS and substrate do not contribute significantly to the overall loss, which is usually the case.

It has been pointed out that the high dielectric constant of the ferroelectric materials can increase the current crowding effect on coplanar lines supported by thin-film ferroelectrics [44]. Current crowding at the edges of the transmission line increases the conductor losses of the line. As the thickness of the film decreases, the field is more confined into the gap between the central conductor and the ground plane [45], further increasing the current crowding. In addition to an increase in losses

due to current confinement at the conductor edges, current crowding effects may also lead to the onset of nonlinearities in HTS film. Such nonlinearities will give rise to increased dissipation and spurious harmonic generation.

It should be noted that the extraction of the dielectric constant from the above expressions is only accurate when both the microwave field and the dc electric field are small. The application of a constant voltage to produce the change in permittivity does not cause the whole of the thin film to have the same permittivity. The bias voltage causes an uneven dc electric field distribution which causes an associated uneven permittivity distribution. A complete calculation of this nonlinear field distribution is required to extract correctly the permittivity and loss tangent values for the higher bias values.

4.2. Microstrip geometry

A number of microstrip resonators have been used for the measurement of the dielectric properties of ferroelectrics. There are three principal types: (1) resonators constructed using a single-crystal substrate with a ground plane deposited on the lower side of the substrate and the signal line on the upper side; (2) a trilayer consisting of a non-ferroelectric substrate, a thin-film conductor ground plane, a thin-film ferroelectric and a thin-film upper conductor; (3) a series capacitor made of thin-film ferroelectric in the centre of a microstrip line. Each of these is discussed briefly below.

An example of one of the few microstrip resonators based on a single-crystal substrate is shown in figure 5 [46–48]. It consists of a circular disk of STO with HTS deposited on each side. The lowest-order resonant mode is TM_{110} which resonates at about 250 MHz for the dimensions shown [48]. Q is about 400 at 40 K, which is limited by losses in the STO film. Q values as high as 10^4 can be expected for good films on good-quality single-crystal STO. The tunability of the mode with the dimensions shown is about 43% for a bias field of 8 kV cm^{-1}. Calculation of the fields and resonant frequency can be based on the assumption that all the fields are confined within the dielectric; however, although the electric field is confined because of the very high dielectric constant of the ferroelectric, the magnetic fringing field becomes the dominant error in this assumption.

The microstrip trilayer is probably the most interesting and most difficult microstrip transmission line or resonator to produce. It is built up as shown in figure 2(b), with the ground plane, ferroelectric and signal plane all composed of thin films. The conducting materials need to be superconductors in order to keep the conductor losses as low as possible. Ultraminiature components can be made this way, since the ferroelectric thickness is typically only of the order of 1 μm. Miniature microstrip filters have already been successfully manufactured using non-ferroelectric, high dielectric constant, dielectric thin films [49]. The theory required to calculate the velocity and impedance on multilayer microstrip structures is fairly straightforward since the transmission line can usually be considered wide with no fringing field at its edges

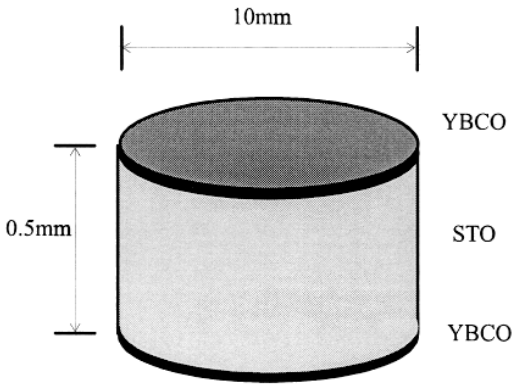

Figure 5. Microstrip disk resonator

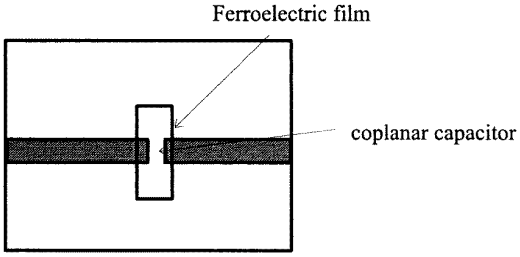

Figure 6. Microstrip resonator with ferroelectric capacitor.

[5, 50, 51]. This follows since the conducting signal strip has to be wider than the 1 μm thickness of the ferroelectric film for practical patterning purposes. A number of tri-layer thin resonators and transmission lines have been constructed and measured [52–55].

An interesting variation on the use of a microstrip transmission line for the measurement of the microwave properties of ferroelectrics is to fabricate a capacitor only at the centre of the transmission line rather than along the whole line [56–58]. This resonator is shown in figure 6. Because of the sinusoidal longitudinal current distribution on the microstrip line, a change in the capacitance of the ferroelectric structure with applied bias only occurs when odd-order resonant modes are excited, leaving the even modes relatively unchanged.

There have been a number of measurements of the properties of materials at high frequencies based on the above resonator techniques. The results are similar to the low-frequency measurements described above. Around 50% tunability can be obtained at both low temperature [32, 48, 58, 59] and room temperature [15, 53, 54] but the loss tangents of the films are generally quite high (in the range 0.01–0.1). A combination of SBT and MgO appears to be promising, with a dielectric constant of 100 and loss tangent of 0.008 at X-band [60]; a tunability of 25% has been observed.

Examples of measurements performed at the University of Birmingham using a coplanar resonator will now be presented. The resonator structure is shown in figure 4. The signal line of the resonator is 8 mm long with a width of 200 μm; the gap between the ground plane and the signal

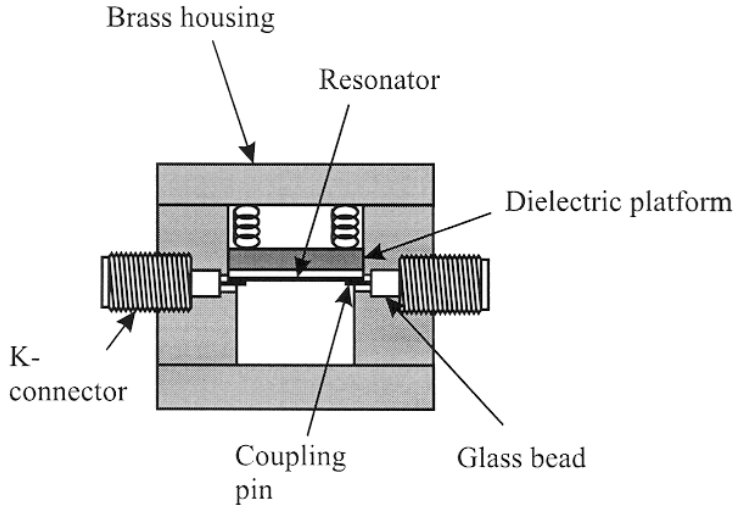

Figure 7. Brass package used to house the coplanar resonator samples.

line is 73 μm. The ground planes are isolated from each other and the outer packaging, so that a dc voltage can be applied across them; this potential is dropped across a total distance of 146 μm. The microwave signal is applied via capacitive coupling, which is weak in order to allow accurate determination of the unloaded quality factor. The packaging of the resonator is shown in figure 7. It consists of a brass box with the device located by a spring onto a ridge. K-connectors are used for the input and output paths for the microwave signals, with the connector pin forming the capacitive coupling.

All the films described below were made by pulsed laser deposition. The films were deposited on 1 cm^2 MgO polished substrates with (100) orientation. The films were deposited at 800 °C in 400 mTorr of oxygen. The STO layers were deposited using approximately 1.7 J cm^{-2} laser fluence at 5 Hz. The YBCO was deposited using 1.5 J cm^{-2} laser fluence for 10 min at 10 Hz, resulting in films about 300 nm thick. Samples were cooled in 1 atm of oxygen with a temperature sweep of 30 °C min^{-1}.

A number of films of varying thickness have been deposited and their properties measured. Prior to patterning of the films into coplanar resonators, the surface resistance (R_S) of the YBCO films was measured at 15 GHz using a dielectric resonator placed on the surface of the unpatterned film [5]. In the dielectric resonator geometry, the microwave fields are effectively screened from the ferroelectric layer by the HTS film above. Therefore, over much of the temperature range, loss measurements are expected to be dominated by the response of the YBCO and not the ferroelectric and dielectric layers beneath it. Figure 8 shows the temperature dependence of the Q factor and the corresponding R_S values at a frequency of 15 GHz. The graph indicates that all the films are similar and are of good quality, irrespective of the STO layer thickness.

Once the quality of the HTS films has been established the coplanar resonator was patterned and measurements made on the ferroelectric thin film. The electric field and temperature dependences of the relative permittivity

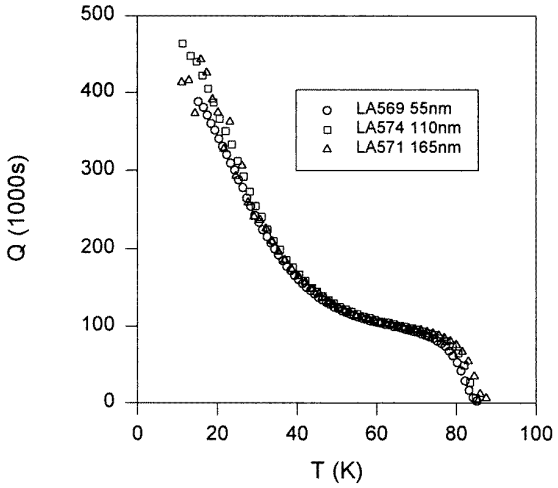

Figure 8. Variation of the unloaded quality factor of the YBCO films using a dielectric resonator at a frequency of 15 GHz. At 40 K the Q shown corresponds to a surface resistance of 0.5 mΩ, increasing to 0.8 mΩ at 77 K for all samples.

of the ferroelectric layer were extracted from the measured resonant frequency. For a fixed resonant length, absolute values of the resonant frequency are determined by the value of the effective dielectric constant, ε_{eff}. ε_{eff} is dependent on the thickness and dielectric constants of the dielectric (ε_D) and ferroelectric (ε_F) films, and can be expressed in terms of these quantities using a conformal mapping technique as explained above.

Absolute values of ε_F can be determined by comparing the absolute resonant frequency of the bilayer structure with that of a film on a bare substrate. Given a single absolute value of ε_F, equation (3) is solved for ε_F at different electric fields (or temperatures) so that measured and theoretical fractional frequency shifts coincide.

Figure 9 shows the fractional frequency shift and values of ε_F, Q factor and $\tan\delta$ for typical bilayer films with

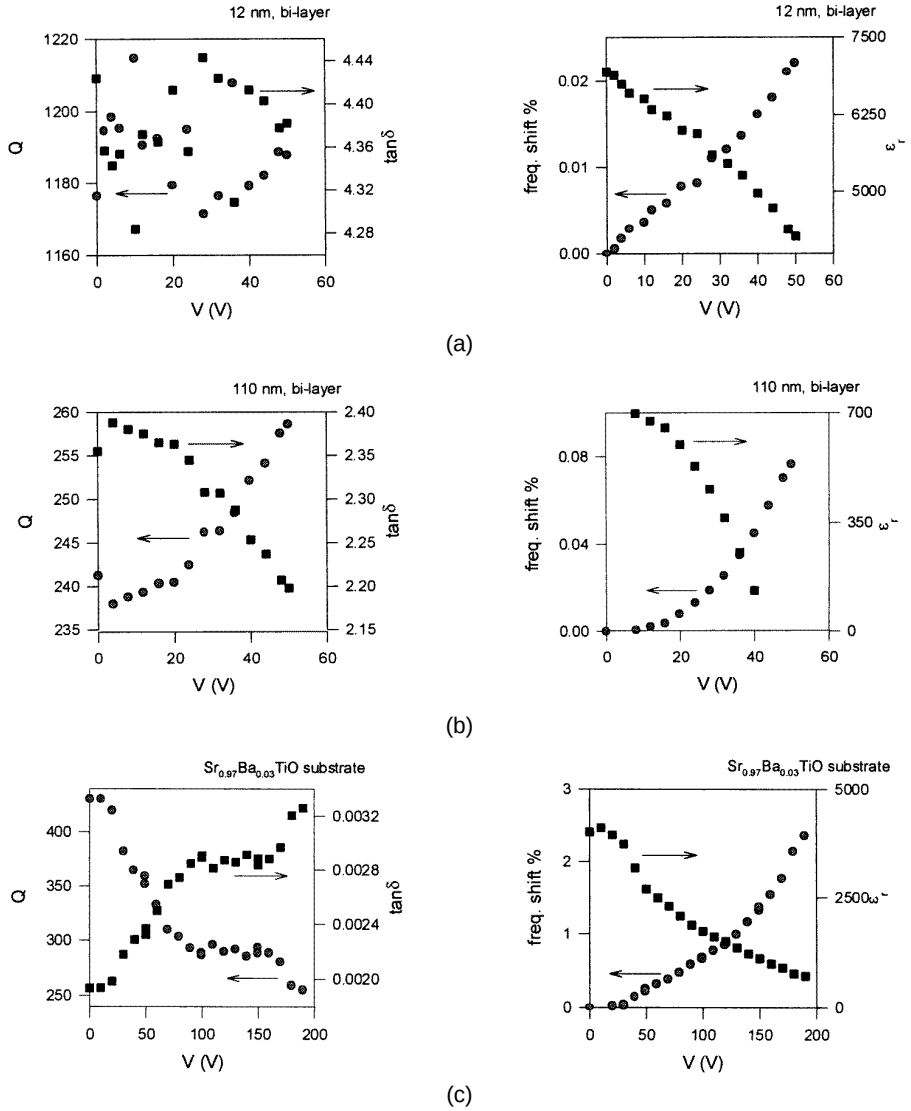

Figure 9. The measured variation in Q, $\tan\delta$, ε_r and frequency shift for (a) 12 nm thick SBT film, (b) 110 nm thick SBT film and (c) 3% barium doped SBT single crystal.

STO layers 12 nm and 110 nm thick and for a film grown on a single-crystal $Sr_{0.97}Ba_{0.03}TiO_3$ substrate. We note that, although a similar functional dependence of ε_F on electrical field is observed for all samples, there is a wide variation in the absolute value of ε_F. Large values of ε_F are observed for samples 1 and 3, where a corresponding overall reduction in the Q factor with electric field is observed. Considerably smaller values of ε_F are observed for sample 2, where an increase in Q with electric field is observed. This might lead us to conclude that samples such as sample 2, which display low values of permittivity and an increase in Q with applied E field, are dominated by the non-intrinsic properties of the ferroelectric layers. However, the electric field dependent fractional frequency shift is similar to that expected using the empirical form of $\varepsilon_F(E)$ discussed above.

Figure 10 shows how the film thickness influences the unloaded quality factor and the maximum frequency shift for a number of different-thickness STO films and the single-crystal SBT. As expected, the thicker films show a greatly reduced Q, owing to most of the electric field being in the lossy ferroelectric; however, in this case a larger frequency shift is available. The converse is true, with a thin film giving a very small frequency shift. It is possible, using this information, to determine an optimum thickness of film for a particular application.

5. Device examples

Despite the large potential of this technology there has been few demonstrations of useful devices. There are a number of reasons for this.

(i) The large loss tangents of the practical ferroelectric materials result in low-Q resonators and lossy delay lines.

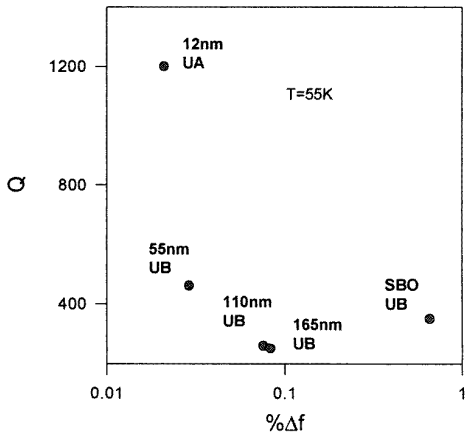

Figure 10. The unloaded quality factor versus the frequency shift with a bias of 50 V (3.5 kV cm^{-1}) for a number of different-thickness films.

(ii) The large dielectric constants result in low-impedance transmission lines and problems with surface wave modes.

(iii) The design of complex bias networks is difficult.

(iv) Large bias voltages are required.

However, a number of microwave circuits have been produced and these are discussed below.

5.1. Phase shifters

The phase shifter is by far the simplest component that can be produced by ferroelectric materials and hence it has been reported by a large number of laboratories. It simply consists of a ferroelectric transmission line of appropriate length. The transmission line must be matched to the external 50 Ω system and have a low loss; it must also have large phase shifts, preferably of 360°, with low applied voltage. Depending on the application, the power requirements may be severe.

By far the most convenient use of ferroelectrics is the room temperature operation of single crystal or polycrystalline materials. However, there have been only few reports of practical devices [61, 62], for the reasons mentioned above. A number of devices have been demonstrated based on thin-film technology [59, 63–65], where the construction is the same as that described above for the microwave measurements using resonators or delay lines; in fact some of the devices described above double as phase shifters. The performance of phase shifters is very variable but shifts greater than 160° at room temperature [63] and low temperature [31, 59, 64] have been reported in both ceramic and thin film forms. Applied voltages remain high but thin film microstrip gives the possibility of a few volts (∼8 V) for reasonable phase shifts (∼80°) [55]. In general, the insertion loss of the phase shifters remains high owing to problems with wideband matching and connections.

5.2. Filters

Despite frequency-agile filters being of paramount importance in microwave systems, surprisingly few ferroelectric filters have been produced. Figure 11 shows three frequency-agile filters based on the use of ferroelectric thin films. Filters have been demonstrated with coplanar, microstrip and waveguide [70] technologies.

Figure 11(a) shows the principle behind a three-pole coplanar filter using thin-film STO 1.2 μm thick on the surface of an $LaALO_3$ crystal [66]. The conductor is YBCO and the whole filter fits in an area of 1 cm^2 with a centre frequency of 2.5 GHz and bandwidth of 2%. Tuning is available on all coupling capacitances and the frequency of each of the three resonators. Results give about a 15% change in centre frequency with an applied voltage of 125 V (4×10^6 V m^{-1}). However, the insertion loss is quite high at 77 K and zero bias (∼16 dB), although this improves at 4 K and maximum bias (∼2 dB).

Figure 11(b) shows a bandstop filter based on a conventional transmission line coupled to a single-crystal STO resonator with YBCO deposited on both sides [67]. The resonator is square rather than the circular one described above. The size is 2 mm square with a thickness of 0.5 mm, and it can be used as a dual-mode resonator. The fundamental resonant frequency is 1 GHz. The configuration shown in figure 11(b) is a bandstop filter with an equivalent circuit of a series resonant element; more elements can be mounted on the line if a more complex filter is required. The centre frequency showed a 50% change with a 500 V bias.

Figure 11(c) shows the layout of a two-pole filter with a 19 GHz centre frequency and a 4% bandwidth [68]. The filter is produced in microstrip. The structure has a gold ground plane, 0.01 in thick $LaAlO_3$ substrate, a 300 nm thick laser-ablated layer of STO and 350 nm of YBCO patterned into the shape shown in figure 11(c). Bias is applied via the points labelled A–C. Because of the nature of the construction, application of bias predominantly changes the coupling between the resonant sections. However, a centre frequency shift of 12% can be obtained with a ±400 V bias at 30 K. The insertion loss is low (<0.5 dB) with a good return loss (< −20 dB). Good passband shape and performance are obtained at 30 K, with degradation as the temperature increases to 77 K.

5.3. Nonlinear applications

In the above discussion a dc or low-frequency bias has been assumed to be applied to the ferroelectric material in order to change its dielectric properties. However, ferroelectric materials respond very rapidly and can react to the microwave signal amplitude itself. The application of the microwave signal itself alters the dielectric constant and therefore the propagation conditions of the signal; this nonlinear effect causes a distortion. For signals of small amplitude this effect is small, but for large-amplitude signals this may be a significant problem.

This nonlinear property of ferroelectrics can be used in principle for many devices, for example harmonic generators, parametric amplifiers, limiters, modulators and

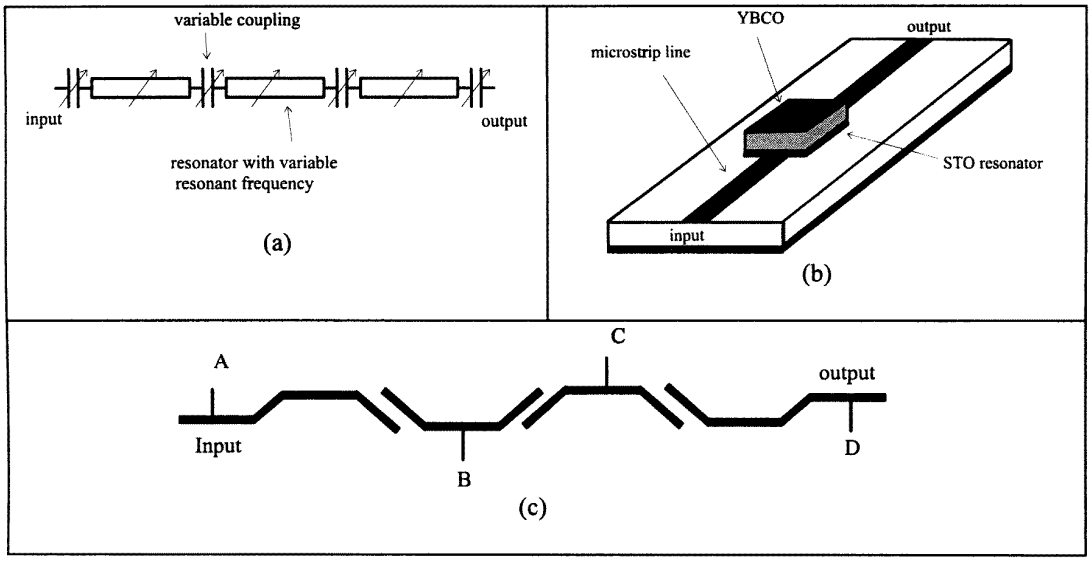

Figure 11. Three ferroelectric filters: (a) coplanar thin-film bandpass filter [66]; (b) single-crystal STO bandstop filter [67]; (c) thin-film microstrip filter [68].

other nonlinear components. For efficient devices, the nonlinear response of the ferroelectric must be large. A harmonic generator using SBT was demonstrated as early as 1961 [71]. This generator operated at a fundamental frequency of 3 GHz with a conversion to 9 GHz using the ferroelectric material. An efficiency of 8.5% with an input power of 2.2 kW was obtained. Although much of the recent device work is not concerned with such high powers, the principle of operation of this generator is of interest to the work today.

It is interesting to consider the propagation of a large-amplitude microwave signal on a transmission line with a ferroelectric material replacing the conventional dielectric material. If a signal is applied to the transmission line at the beginning of the microwave cycle, the electric field is small so the signal travels at a velocity $c = 1/(LC)^{1/2}$, where L and C are the inductance and capacitance per unit length of the transmission line. As the voltage increases in the cycle, the increased field reduces the dielectric constant of the material, having the effect of reducing the capacitance. This reduction in capacitance gives an increase in the velocity and hence larger signal levels within the microwave signal travel faster. The peak of the sine wave therefore travels faster, thus catching up with the low-level parts. The result is a distortion of the shape of the microwave signal from a sine wave towards a shock front [72]. The larger the propagation distance the larger the effect and the more distorted the signal becomes. During this process energy is being transferred from the fundamental frequency into harmonic frequencies. If two signals are applied to the transmission line then mixing occurs.

To understand how the nonlinear mixing occurs consider the basic transmission line equations

$$\frac{\partial i(z,t)}{\partial z} = -\frac{\partial [C(v)v(z,t)]}{\partial t} \qquad \frac{\partial v(z,t)}{\partial z} = -L\frac{\partial [i(z,t)]}{\partial t}$$

where i and v are the microwave current and voltage at distance z and time t on the transmission line. The nonlinear capacitance can be expanded as a Taylor series

$$C(v) = c_0 + c_1 v + c_2 v^2 + \cdots$$

where the coefficients c_0, c_1, $c_2 \ldots$ are dependent on the ferroelectric material. If voltages $v_p \cos(\omega_p t)$ and $v_s \cos(\omega_s t)$ are applied to the transmission line then it can be shown that the power converted into the frequencies $\omega_p \pm \omega_s (\omega_p > \omega_s)$ is given by [73, 74]

$$P_{p\pm s} \approx \frac{1}{2} P_p P_s Z_0 \beta_{p\pm s} \beta_s l^2 \frac{\omega_p \pm \omega_s}{\omega_s} \left(\frac{c_1}{c_0}\right)^2.$$

Here P represents the input signal powers (assumed equal), β is the propagation constant, Z_0 is the transmission line impedance and l the length of the transmission line. It can be seen that even with low power it is possible to obtain mixing if the transmission line is long enough. Thin-film STO and SBT coplanar transmission lines with HTS and Au electrodes have been shown to produce this mixing effect at room temperature and 77 K respectively [31, 74].

6. Conclusion

The potential of ferroelectric materials (particularly STO and SBT) for microwave applications has been known for many decades. However, it is only recently that interest has developed to a stage that practical devices have been demonstrated. The reason for the recent activity is the compatibility of ferroelectrics with HTS materials. Although HTS is not necessary for the demonstration of useful devices, integration of the two technologies gives the potential for a number of miniature and highly functional components. A wide range of materials has been produced and some excellent-quality thin-film, polycrystalline and single-crystal, ferroelectrics have been obtained. The problem of the high loss tangent still remains the main

obstacle to exploitation, but the lower loss of single crystals gives some optimism for a reduction of the loss tangent of thin films in the future. Work on doping and new materials will continue, and there is no reason why better materials cannot be produced.

Acknowledgments

The authors would like to acknowledge support from the Nuffield Foundation for support of Dr Lancaster. In addition, the support from EPSRC for this work is acknowledged.

References

[1] Xu Y 1991 *Ferroelectric Materials* (New York: Elsevier)
[2] 1964 Microwave ferroelectric phase shifters and switches *US Army Final Report* Contract DA 36-039-AMC-02340 (E) US Army Electronics Laboratories, Fort Monmouth, NJ, USA
[3] Rupprecht G and Bell P O 1962 Microwave losses in strontium titanate above the phase transition *Phys. Rev.* **123** 1915–20
[4] Dionne G F, Oates D E and Temme D H 1995 YBCO/ferrite low loss microwave phase shifter *IEEE Trans. Appl. Supercond.* **5** (2) 2083–6
[5] Lancaster M J 1997 *Passive Microwave Device Applications of High Temperature Superconductors* (Cambridge: Cambridge University Press)
[6] Jackson C M, Kobayashi J H, Guillory E B, Perriete-Hall C L and Burch J F 1992 Monolithic HTS microwave phase shifter and other devices *J. Supercond.* **5** (4) 419–24
[7] Wu H D, Harsh K F, Irwin R S, Zhang W, Mickelson A R and Lee Y C 1998 MEMS designed for tunable capacitors *IEEE MTT-S Dig.* **1** 127–9
[8] Herner S B, Selmi F A, Varadan V V and Varadan V K 1993 The effect of various dopants on the dielectric properties of barium strontium titanate *Mater. Lett.* **15** 317–24
[9] Jackson C M, Kobayashi J H, Lee A, Prentice-Hall C, Burch J F and Hu R 1992 Novel monolithic phase shifter combining ferroelectrics and high temperature superconductors *Microwave Opt. Technol. Lett.* **5** 722–6
[10] Selmi F, Guerin F, Yu X D, Varadan V K and Varadan V V 1992 Microwave calcination and sintering of barium strontium titanate *Mater. Lett.* **12** 424–8
[11] Vendik O G 1976 Dielectric nonlinearity of the displacive ferroelectric at UHF *Ferroelectrics* **12** 85–90
[12] Neville R C, Hoeneisen B and Mead C A 1972 Permittivity of strontium titanate *J. Appl. Phys.* **43** 2124–31
[13] Boikov Y A, Ivanov Z G, Vasiliev A L and Claeson T 1995 Epitaxial $YBa_2Cu_3O_{7-\delta}/Ba_xSr_{1-x}TiO_3$ heterostructures on silicon-on-sapphire for tunable microwave components *J. Appl. Phys.* **78** 4591–5
[14] Poplavko Y M, Tsykalov V G and Molchanov V I 1969 Microwave dielectric dispersion of the ferroelectric and parametric phases of barium titanate *Sov. Phys–Solid State* **10** (11) 2708–10
[15] De Flavis F, Chang D, Alexopoulos N G and Stafsudd O M 1996 High purity ferroelectric materials by sol-gel process for microwave applications *IEEE MTT-S Int. Microwave Symp.* pp 99–102
[16] Sengupta L, Ngo E, Stowell S, O'Day M and Lancto R 1995 Ceramic ferroelectric composite material—BSTO-MGO *United States Patent* 5 427 988, 27 June 1995
[17] Boikov Y A and Claeson T 1997 High tunability of the permittivity of $YBa_2Cu_3O_{7-\delta}/SrTiO_3$ heterostructures on sapphire substrates *J. Appl. Phys.* **81** (7) 3232–6
[18] Miranda F A, Mueller C H, Cubbage C D, Bhasin K B, Sing R K and Harkness S D 1995 HTS/ferroelectric thin films for tunable microwave components *IEEE Trans. Appl. Supercond.* **5** (2) 3191–4
[19] Miranda F A, Mueller C H, Koepf G A and Yandrofski R M 1995 Electrical response of ferroelectric/superconducting/dielectric $Ba_xSr_{1-x}TiO_3/YBa_2Cu_3O_{7-\delta}/LaAlO_3$ thin-film multilayer structures *Supercond. Sci. Technol.* **8** 755–63
[20] Boikov Y A, Ivanov Z G, Vasiliev A L, Olsson E and Claeson T 1996 Epitaxial heterostructures of $YBa_2Cu_3O_{7-\delta}/KTaO_3$ and $YBa_2Cu_3O_{7-\delta}/Ba_xSr_{1-x}TiO_3$ for tunable microwave components *Supercond. Sci. Technol.* **9** A178–81
[21] Treece R E, Thompson J B, Mueller C H, Rivkin T and Cromar M W 1997 Optimisation of $SrTiO_3$ for applications in tunable resonant circuits *IEEE Trans. Appl. Supercond.* **7** (2) 2363–6
[22] Gevorgian S, Carlsson E, Rudner S, Wernlund L-D, Wang X and Helmersson U 1996 Modelling of thin-film HTS/ferroelectric interdigital capacitors *IEE Proc. Microwave Antennas Propag.* **143** (4) 397–401
[23] Wu H-D, Zhang Z, Barnes F, Jackson C M, Kain A and Cuchiaro J D 1994 Voltage tuneable capacitors using high temperature superconductors and ferroelectrics *IEEE Trans. Appl. Supercond.* **4** (3) 156–9
[24] Krupka J, Geyer R G, Khun M and Hinken J H 1994 Dielectric properties of single crystals of Al_2O_3, $LaAlO_3$, $NdGaO_3$ $SrTiO_3$ and MgO at cryogenic temperatures *IEEE Trans. Microwave Theory Tech.* **42** (10) 1886–90
[25] Syamaprasad U R K, Galgali R K and Mohanty B C 1988 Dielectric properties of $Ba_{1-x}Sr_xTiO_3$ system *Mater. Lett.* **7** 197–200
[26] Silverman B D 1964 Temperature dependence of the frequency spectrum of parametric materials *Phys. Rev.* A **135** 1596–603
[27] Silverman B D 1962 Microwave absorption in cubic strontium titanate *Phys. Rev.* **125** (6) 1921–30
[28] Gevorgian S, Kaparkov I and Vendik O G 1994 Electrically controlled HTSC/ferroelectric coplanar waveguide *IEE Proc. Microwave Antennas Propag.* **141** (6) 501–3
[29] Vendik O G, Ter-Martirosyan L T and Zubko S P 1998 Microwave losses in incipient ferroelectrics as functions of temperature and biasing field *J. Appl. Phys.* **84** 993–8
[30] DeGroot D G, Beall J A, Marks R B and Rudman D A 1995 Microwave properties of voltage-tunable $YBa_2Cu_3O_{7-\delta}/SrTiO_3$ coplanar waveguide transmission lines *IEEE Trans. Appl. Supercond.* **5** (2) 2272–5
[31] Findkoglu A T, Jia Q X and Reagor D W 1997 Superconductor/non-linear dielectric bilayers for tunable and adaptive microwave devices *IEEE Trans. Appl. Supercond.* **7** (2) 2925–8
[32] Findikoglu A T, Jia Q X, Campbell I H, Wu X D, Reagor D, Mombourquette C B and McMurry D 1995 Electrically tunable coplanar transmission line resonators using $YBa_2Cu_3O_{7-x}/SrTiO_3$ bilayers *Appl. Phys. Lett.* **66** (26) 3674–6
[33] Hermann A M, Price J C, Scott J E, Yandrofski R M, Naziripour A, Galt D, Paranthaman H M, Tello R, Cuchario J and Ahrenkiel R K 1993 Tuneable microwave resonators utilising thin high temperature superconducting films and ferroelectrics *Bull. Am. Phys. Soc.* **38** 689–92
[34] Porch A, Lancaster M J and Humphreys R 1995 Coplanar resonator technique for the determination of the surface impedance of patterned thin films *IEEE Trans. Microwave Theory Tech.* **43** (2) 306–14
[35] Silvester P 1968 TEM wave properties of microstrip transmission lines *Proc. IEE* **115** (1) 43–8

[36] Wen C P 1969 Coplanar waveguide: A surface strip transmission line suitable for nonreciprocal gyromagnetic device applications *IEEE Trans. Microwave Theory Tech.* **17** (12) 1087–90
[37] Hilberg W 1969 From approximations to exact relations for characteristic impedances *IEEE Trans. Microwave Theory Tech.* **17** 259–65
[38] Davis M E, Williams E W and Celestini A C 1973 Finite-boundary corrections to the coplanar waveguide analysis *IEEE Trans. Microwave Theory Tech.* **23** 594–6
[39] Veyres C and Hanna V F 1980 Extension of the application of conformal mapping techniques to coplanar lines with finite dimensions *Int. J. Electron.* **48** (1) 47–56
[40] Zhu N H, Pun E Y B and Li J X 1995 Analytical formulas for calculating the effective dielectric constant of coplanar lines for OIC applications *Microwave Opt. Technol. Lett.* **9** (4) 229–32
[41] Gevorgian S S 1994 Basic characteristics of two layered substrate coplanar waveguides *Electron. Lett.* **30** (15) 1236–7
[42] Chen E and Chou S Y 1997 Characteristics of coplanar transmission lines on multilayer substrates: modelling and experiments *IEEE Trans. Microwave Theory Tech.* **45** (6) 939–45
[43] Findikoglu A T, Jia Q X, Reagor D W and Wu X D 1995 Electrical characteristics of coplanar waveguide devices incorporating non-linear dielectric thin films of $SrTiO_3$ and $Sr_{0.5}Ba_{0.5}TiO_3$ *Microwave Opt. Technol. Lett.* **9** (6) 306–8
[44] Carlsson E and Gevorgian S 1997 Effect of enhanced current crowding in a CPW with a thin ferroelectric film *Electron. Lett.* **33** (2) 145–6
[45] Carlsson E and Gevorgian S 1998 Conformal mapping of the field and charge distributions in multilayered substrate CPW's *IEEE Microwave Theory Tech.* submitted
[46] Gevorgian S S, Carlsson E F, Rudner S, Helmersson U, Kollberg E L, Wikbourg E and Vendik O G 1997 HTS/ferroelectric devices for microwave applications *IEEE Trans. Appl. Supercond.* **7** (2) 2458–62
[47] Vendik O G, Kollberg E, Gevorgian S S, Kozyrev A B and Soldatenkov O I 1995 1 GHz tunable resonator on bulk single crystal $SrTiO_3$ plated with $YBa_2Cu_3O_{7-x}$ films *Electron. Lett.* **31** (8) 654–6
[48] Gevorgian S, Carlsson E, Linner P, Kolberg E, Vendik O and Wikborg E 1996 Lower order modes of YBCO/STO/YBCO circular disk resonators *IEEE Trans. Microwave Theory Tech.* **44** (10) 1738–41
[49] Carroll K R, Pond J M and Cukauskas E J 1993 Superconducting kinetic inductance microwave filters *IEEE Trans. Appl. Supercond.* **3** (1) 8–16
[50] Abbas F, Davis L E and Gallop J C 1995 Tunable microwave components based on dielectric nonlinearity by using HTS/ferroelectric thin films *IEEE Trans. Appl. Supercond.* **5** (4) 3511–17
[51] Abbas F, Davis L E and Gallop J C 1996 A distributed ferroelectric superconducting transmission-line phase shifter *IEEE MTT-S Int. Microwave Symp.* 1671–4
[52] Findikoglu A T, Doughty C, Anlage S M, Li Q, Xi X X and Venkatesan T 1993 Effect of dc electric field on the effective microwave surface impedance of $YBa_2Cu_3O_7/SrTiO_3/YBa_2Cu_3O_7$ trilayers *Appl. Phys. Lett.* **63** (23) 3215–17
[53] Carroll K R, Pond J M, Chrisey D B, Horwitz J S, Leuchtner R E and Grabowski K S 1993 Microwave measurement of the dielectric constant of $Sr_{0.5}Ba_{0.5}TiO_3$ ferroelectric thin films *Appl. Phys. Lett.* **62** (15) 1845–7
[54] Carroll K R, Pond J M, Chrisey D B, Horwitz J S, Leuchtner R E and Grabowski K S 1993 Erratum. Microwave measurement of the dielectric constant of $Sr_{0.5}Ba_{0.5}TiO_3$ ferroelectric thin films *Appl. Phys. Lett.* **63** (9) 1291
[55] Chrisey D B, Horwitz J S, Pond J M, Carrol K R, Lubitz P, Grabowski K S, Leuchtner R E, Carosella C A and Vittoria C V 1993 Pulsed laser deposition of novel HTS multilayers for passive and active device applications *IEEE Trans. Appl. Supercond.* **3** (1) 1528–31
[56] Galt D, Price J C, Beall J A and Ono R H 1993 Characterisation of tunable thin film microwave $YBa_2Cu_3O_{7-x}/SrTiO_3$ coplanar capacitor *Appl. Phys. Lett.* **63** (22) 3078–080
[57] Beall J, Ono R H, Galt D and Price J C 1993 Tunable high-temperature superconductor microstrip resonators *IEEE MTT-S Int. Microwave Symp. Digest* 1421–3
[58] Galt D, Price J C, Beall J A and Harvey T E 1995 Ferroelectric thin film characterisation using superconducting microstrip resonators *IEEE Trans. Appl. Supercond.* **5** (2) 2575–8
[59] Jackson C M, Pham T, Zhang Z, Lee A and Pettiete-Hall C 1995 Model for a novel CPW phase shifter *IEEE MTT-S Int. Microwave Symp.* 1439–42
[60] Rao J B L and Patel D P 1998 Phased array antennas based on bulk phase shifting with ferroelectrics *Workshop on Technologies for Tunable Microwave Systems, IEEE MTT-S IMS*
[61] http://horse.arl.mil/ferro/ferro.hmtl
[62] Collier D C 1998 Ferroelectric phase shifters for phased array radar applications *IEEE MTT-S IMS* 199–201
[63] De Flaviis F, Alexopoulos N G and Stafsudd O M 1997 Planar microwave integrated phase-shifter design with high purity ferroelectric material *IEEE Trans. Microwave Theory Tech.* **45** (6) 963–9
[64] Vendik O G, Varlsson E F, Petrov P K, Chakalov R A, Gevorgian S S and Ivanov Z G 1997 HTS/ferroelectric CPW structures for voltage tunable phase shifters *EuMC Jerusalem* 196–202
[65] Chakalov R A, Ivanov Z G, Boikov Y A, Larsson P, Carlsson E and Gevorgian S 1997 Investigation of voltage tuneable phase shifters based on HTSC/ferroelectric thin film coplanar waveguides *European Conf. Appl. Supercond.*
[66] Findikoglu A T, Jia Q X, Wu X D, Chan G J, Venkatesan T and Reagour D W 1996 Tunable and adaptive bandpass filter using non-linear dielectric thin film of $SrTiO_3$ *Appl. Phys. Lett* **68** (12) 1651–3
[67] Gevorgian S, Carlson E, Kollberg E and Wikborg E 1998 Tunable superconducting bandstop filters *IEEE MTT-S Digest* 1027–30
[68] Subramanyam G, Keuls F V and Miranda F A 1998 A novel K-band tunable microstrip bandpass filter using a thin film HTS/ferroelectric/dielectric multilayer configuration *IEEE MTT-S Digest* 1011–14
[69] Varadan V K, Ghodgaonkar D K, Varadan V V, Kelly J F and Glikerdas P 1992 Ceramic phase shifters for electronically steerable antenna systems *Microwave J.* **35** (January) 116 *et seq*
[70] Kozyrev A *et al* 1998 Ferroelectric films: nonlinear properties and applications in microwave devices *IEEE MTT-S IMS Digest* 985–8
[71] DiDomeniko M, Johnson D and Pantell R 1962 Ferroelectric harmonic generator and large-signal microwave characteristics of a ferroelectric ceramic *J. Appl. Phys.* **33** 1697–706
[72] Wilson C R, Turner M M and Smith P W 1990 Electromagnetic shock-wave generation in a lumped element delay line containing non-linear ferroelectric capacitors *Appl. Phys. Lett.* **56** (24) 2471–3
[73] Tien P K 1958 Parametric amplification and frequency mixing in propagating circuits *J. Appl. Phys.* **29** (9) 1347–57
[74] Findikoglu A T, Jia Q X, Reagor D W and Wu X D 1995 Tunable microwave mixing in non-linear dielectric thin films of $SrTiO_3$ and $Sr_{0.5}Ba_{0.5}TiO_3$ *Electron. Lett.* **31** (21) 1814–15